



Supporting Online Material for
**Major Galaxy Mergers and the Growth of Supermassive Black Holes in
Quasars**

Ezequiel Treister,* Priyamvada Natarajan,* David B. Sanders, C. Megan Urry, Kevin
Schawinski, Jeyhan Kartaltepe

*To whom correspondence should be addressed. E-mail: treister@ifa.hawaii.edu (E.T.);
priyamvada.natarajan@yale.edu (P.N.)

Published 25 March 2010 on *Science Express*
DOI: 10.1126/science.1184246

This PDF file includes:

SOM Text
Figs. S1 and S2
References

Supporting Online Material “Galaxy Mergers and the Growth of SuperMassive Black Holes”

E. Treister et al.

Observations of obscured quasars

Finding obscured sources is a difficult task. So difficult that in fact for a while it was suspected that these sources did not exist. However, now mostly due to extensive multiwavelength surveys a significant number of these sources have been identified. In this work, we have compiled observations of obscured quasars selected at various wavelengths using different techniques, which are described below.

In the nearby Universe, we can estimate the number of heavily-obscured quasars from the space density of ULIRGs. In particular, we base our calculation in the IRAS Revised Bright Galaxy Sample (*S15*). This sample includes both obscured and unobscured quasars, since only an IR selection was done. A random subsample of 16 sources with $L_{\text{IR}} > 10^{12} L_{\odot}$ was observed in X-rays by *Chandra* (*S9*). Of those, 9 have clear AGN signatures, namely a flat X-ray spectrum, and hence the fraction of AGN in this ULIRG sample is at least 56%. However, for the remaining 7 sources a strong Fe K emission lines is detected in the stacked X-ray signal. Since detection of Fe K in emission is considered an unambiguous AGN signature, we can conclude that the fraction of sources containing an AGN, even in the sample of 7 sources not dominated by the AGN emission, should be very high. Similarly, although at higher redshifts, from a sample of 70 μm -selected sources in the Cosmic Evolution Survey (COSMOS) field detected with *Spitzer*, J. Kartaltepe et al. (*S11*) conclude that the fraction of sources with AGN signatures at $L_{\text{IR}} > 10^{12} L_{\odot}$ is higher than 80% and 100% for $L_{\text{IR}} > 10^{13} L_{\odot}$. Hence, our

assumption that most (if not all) of the ULIRGs contain an AGN is well justified.

Heavily-obscured quasars can in principle be selected by their X-ray emission. The effects of obscuration are more important at softer energies, while harder X-ray photons can in principle escape more easily. This is why it is possible to study even Compton-thick sources at high redshifts using the Chandra bands, which trace rest-frame energies >10 keV at $z>1$. There are two types of Compton-thick quasars based on their X-ray spectra: transmission-dominated sources, characterized by a photoelectric cutoff at $E\sim 10$ keV corresponding to a $N_H\sim 10^{24}$ cm $^{-2}$ and in which the intrinsic emission is visible at higher energies, and reflection-dominated quasars, which are in general more obscured sources in which the intrinsic emission at X-ray wavelengths is completely absorbed and only a weak (~ 1 -2% of the intrinsic luminosity) reflection component can be detected.

Using the deep Chandra observations available in the Chandra Deep Field South (CDF-S), P. Tozzi et al. (*S17*) identified 10 Compton-thick candidates (both transmission and reflection dominated) with intrinsic luminosity $L_X > 10^{44}$ erg/s in the $0.73 < z < 4.29$ range. These sources were used to compute the space density of Compton-thick AGN in two redshift bins at $z\sim 1$ and $z\sim 2$, as shown in Fig. 1 in the main text.

As most of the absorbed energy is re-radiated at infrared wavelength, obscured AGN are in general very bright in the mid-IR bands (e.g., *S18*). Using a combination of optical and mid-IR spectroscopy, together with X-ray data, seven Compton-thick quasar candidates at $z\sim 2$ were identified (*S1*). The space density of Compton-thick quasars was estimated by these authors from the four sources found in the GOODS-North field to be $\simeq 0.7$ - 2.5×10^{-5} Mpc $^{-3}$.

Using a method based only on optical to mid-IR photometry, F. Fiore et al. (*S3*) showed that the sources with a high mid-IR to optical flux ratio present at the same time significant X-ray emission, higher than the expected value for pure star-forming galaxies and consistent with Compton-thick obscuration levels. This selection method was then applied to the sources in the COSMOS field (*S4*). This provides a space density of Compton-thick quasars of $4.8 \pm 1.1 \times 10^{-6}$ Mpc $^{-3}$ in the $1.2 < z < 2.2$ redshift bin. As can be seen in Fig. 1 of the main paper, this value is in very good agreement with the density derived from X-ray observations (*S17*) for sources at similar redshifts using a completely independent selection technique.

The same optical to mid-IR selection technique was used in the Extended

CDF-S (ECDF-S) field (S19), which has very deep *Spitzer* and *Chandra* imaging over a $\sim 0.3 \text{ deg}^2$ region of the sky. A total of 211 Compton-thick quasar candidates were found using the selection scheme of F. Fiore et al. (S3). Thanks to the larger number of sources in this sample, it is possible to measure the density of heavily-obscured sources in four redshift bins, from $z \sim 1.5$ to $z \sim 2.9$.

Estimating the ratio of obscured to unobscured quasars from galaxy mergers

In order to calculate the redshift dependence of the ratio of obscured to unobscured quasars we start with the following reasonable and justifiable assumptions. New quasars are ignited by the gas-rich merger of two massive galaxies. The product of this merger produces a ULIRG, which harbors at its center a heavily-obscured quasar. After a time Δt most of the surrounding dust and gas are blown out by the radiation pressure of the rapid on-going accretion, after which an unobscured optically bright quasar is visible. In this scenario, the ratio of obscured to unobscured quasars as a function of redshift is simply given by the merger rate of gas-rich galaxies (equation 1) in the main text of the paper. Here, we describe and evaluate each term in that equation and its redshift dependence in detail.

One of the fundamental ingredients in this calculation is the evolution of the merger rate and its dependence on other parameters like e.g., galaxy mass. This is still a controversial topic. While work based on galaxy morphology to identify mergers reported no redshift dependence (e.g., S12), others based on galaxy pairs (e.g., S10) found a strong redshift dependence of the form $\simeq (1+z)^3$. A compilation by P. Hopkins et al. (S7), which includes the sources in the two samples mentioned before, concluded that once the differences in median galaxy mass and mass ratio (minor versus major mergers) are accounted for, the dependence of the merger rate on redshift is confirmed at a high statistical significance. Following this work, the major merger rate per galaxy as derived from simulations constrained by observations is parametrized as:

$$\frac{d^2 \text{Merger}}{dt dN} = A(M_{\text{Min}})(1+z)^{\beta(M_{\text{Min}})} \quad (1)$$

where

$$A(M_{\text{Min}}) = 0.02[1 + (\frac{M}{2 \times 10^{10} M_{\odot}})^{0.5}] \text{ Gyr}^{-1}$$

and

$$\beta(M_{\text{Min}}) = 1.65 - 0.15 \log(\frac{M}{2 \times 10^{10} M_{\odot}}).$$

Uncertainties in these parameters are a factor of ~ 2 in $A(M_{\text{Min}})$ and 0.2 in $\beta(M_{\text{Min}})$. The minimum stellar mass in our definition of “massive” galaxy is a function of redshift, as shown in Fig. S1, and can be parametrized as

$$M_{\text{Min}}(z) = 5 \times 10^{11} (1 + z)^{-1.5} M_{\odot}. \quad (2)$$

Hence, $A(M)$ ranges from 0.12 Gyrs^{-1} at $z=0$ to 0.06 Gyrs^{-1} at $z=3$, while $\beta(M)$ goes from 1.44 at $z=0$ to 1.58 at $z=3$. The resulting redshift dependence of the merger rate per galaxy is shown in Fig. S2.

The space density of galaxies as a function of stellar mass and redshift was determined observationally recently by D. Marchesini et al. (*S13*). They report that the stellar mass function is well-fit by a Schechter (*S16*) function up to $z \sim 4$ in which the normalization is a function of redshift. To calculate the merging rates of massive galaxies, we use the limiting stellar mass given by equation (2). The resulting space density of massive galaxies as a function of redshift is shown by the blue line on Fig. S2. In order to estimate the number of gas-rich galaxies the extinction-corrected star formation rate density as a function of redshift is used as a proxy of available gas mass at each epoch. This is done because direct measurements of gas contents, especially in high redshift galaxies, are very difficult and hence we have to rely on secondary indicators. In particular, we use the measurements obtained from the Great Observatories Origins Deep Survey (GOODS) observations (*S2*). A good fit to these data, normalized to the high-redshift value, is obtained using the following expression

$$\text{Gas rich}(z) = \begin{cases} 0.11(1+z)^{2.0} & z \leq 2 \\ 1 & z > 2 \end{cases}. \quad (3)$$

This dependence (shown in Fig. S2) is consistent with results obtained from hydrodynamical simulations (*S6*). Finally, the number of unobscured quasars is obtained directly from observations, in particular from X-ray luminosity functions (*S5*). Since this selection was made at soft X-ray energies,

this ensures that only unobscured sources are included. Only sources with $L_X > 10^{44}$ erg/s, corresponding to $L_{\text{bol}} > 10^{45}$ erg/s, were considered. If instead an optical luminosity function (e.g., S14) is used, assuming in this case an equivalent magnitude cut of $M_i < -23$ corresponding to a similar luminosity threshold, the results are consistent. As can be seen in Fig. S2, the quasar number density has a strong peak at $z \sim 1.5$, followed by a shallow decline towards higher redshifts.

The redshift dependence of each of the components in our calculation is shown in Fig. S2. Both the number of unobscured quasars and massive galaxies show steep declines from $z \sim 1$ to $z = 0$. Meanwhile, the merger rate increases steadily by a factor of ~ 3 from $z = 0$ to $z = 3$.

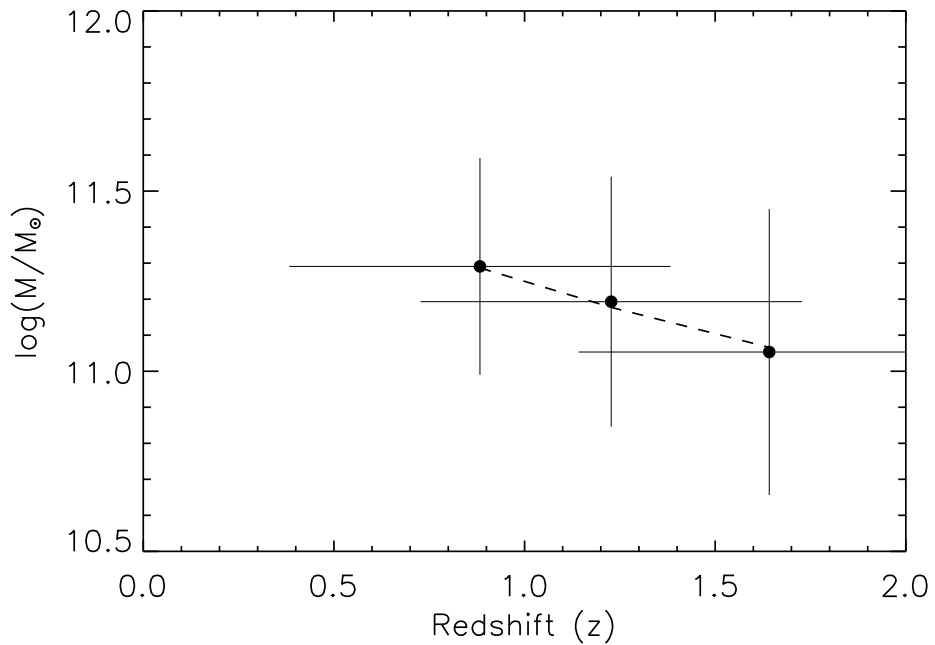


Figure 1: Median stellar mass as a function of redshift for the host galaxies of the ULIRGs ($L_{\text{IR}} > 10^{12} L_{\odot}$) in the COSMOS field. Stellar masses were derived by performing spectral fitting of the observed-frame optical and near-IR photometric data (*S8*). Vertical error bars were obtained from the dispersion in each bin, while the horizontal error bar show the width of each bin. The dashed line shows the best-fitting power-law, $5 \times 10^{11} (1+z)^{-1.5} M_{\odot}$, which is used to compute the number of galaxies hosting ULIRGs as a function of redshift.

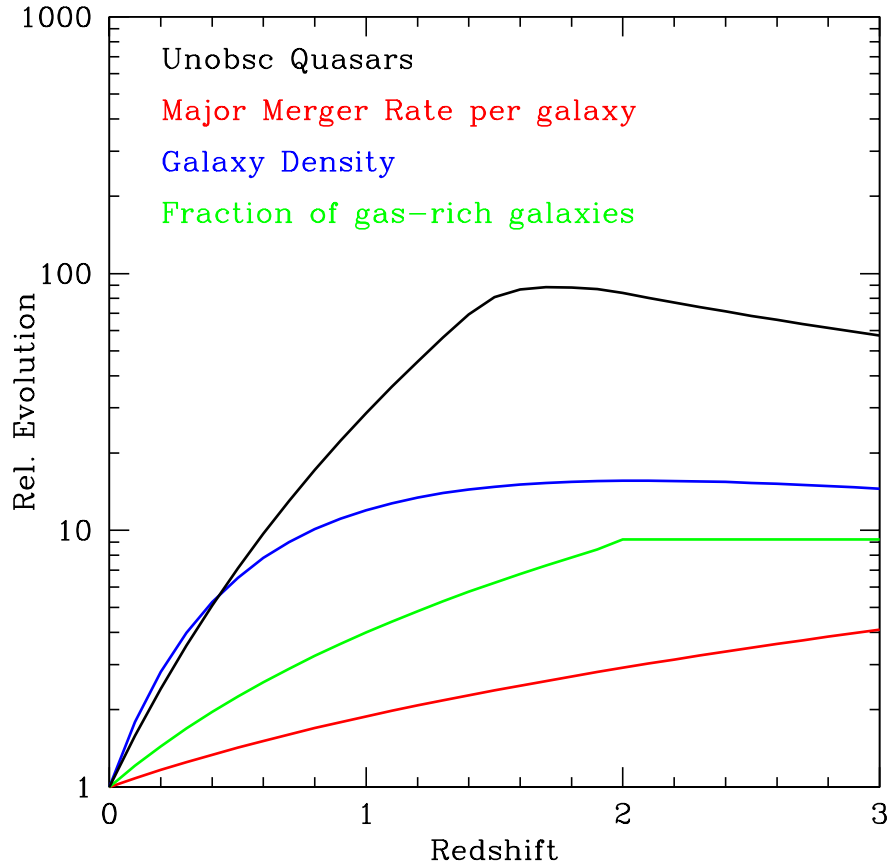


Figure 2: Evolution of the different ingredients used in our calculation of the expected ratio of obscured to unobscured quasars as a function of redshift. All curves were normalized to their $z=0$ value. *Black line* shows the evolution of the density of unobscured quasars, while the redshift dependence of the major merger frequency per galaxy, density of massive galaxies and fraction of gas-rich galaxies is shown by the *red*, *blue* and *green* lines.

References

- S1. Alexander, D. M., et al. 2008, ApJ, 687, 835
- S2. Dahlen, T., Mobasher, B., Dickinson, M., Ferguson, H. C., Giavalisco, M., Kretchmer, C., & Ravindranath, S. 2007, ApJ, 654, 172
- S3. Fiore, F., et al. 2008, ApJ, 672, 94
- S4. Fiore, F., et al. 2009, ApJ, 693, 447
- S5. Hasinger, G., Miyaji, T., & Schmidt, M. 2005, A&A, 441, 417
- S6. Hopkins, P. F., Hernquist, L., Cox, T. J., Robertson, B., & Krause, E. 2007, ApJ, 669, 45
- S7. Hopkins, P. F., et al. 2009, arXiv:0906.5357
- S8. Ilbert, O., et al. 2010, ApJ, 709, 644
- S9. Iwasawa, K., Sanders, D. B., Evans, A. S., Mazzarella, J. M., Armus, L., & Surace, J. A. 2009, ApJ, 695, L103
- S10. Kartaltepe, J. S., et al. 2007, ApJS, 172, 320
- S11. Kartaltepe, J. S., et al. 2010, ApJ, 709, 572
- S12. Lotz, J. M., et al. 2008, ApJ, 672, 177
- S13. Marchesini, D., van Dokkum, P. G., Förster Schreiber, N. M., Franx, M., Labbé, I., & Wuyts, S. 2009, ApJ, 701, 1765
- S14. Richards, G. T., et al. 2006, AJ, 131, 2766
- S15. Sanders, D. B., Mazzarella, J. M., Kim, D.-C., Surace, J. A., & Soifer, B. T. 2003, AJ, 126, 1607
- S16. Schechter, P. 1976, ApJ, 203, 297
- S17. Tozzi, P., et al. 2006, A&A, 451, 457
- S18. Treister, E., et al. 2006, ApJ, 640, 603
- S19. Treister, E., et al. 2009, ApJ, 706, 535